Int. J. Multiphase Flow Vol. 15, No. 1, pp. 65–79, 1989
Printed in Great Britain.

0301-9322/89 $3.00 + 0.00

AXIAL VOID DISTRIBUTION IN TWO LATERALLY INTERCONNECTED CHANNELS WITH BLOCKAGES

A. TEYSSEDOU,[1] A. TAPUCU,[1] M. GEÇKINLI[2] and M. MERILO[3]
[1]Ecole Polytechnique, 2900 Eduard Montpetit, Montréal, Québec H3T 1J4, Canada
[2]Technical University of Istanbul, Ayazaga Kampusu, Masalak, Istanbul, Turkey
[3]Electric Power Research Institute, California, U.S.A.

(*Received* 27 *July* 1988; *in revised form* 8 *September* 1988)

Abstract—In this research the axial void fraction distribution in two laterally interconnected channels with plate or smooth blockages in one of them has been determined experimentally for different void conditions at the inlet of the blocked and unblocked channels. It is observed that a substantial recirculation zone with high void content forms downstream of the blockage. Outside of this recirculation zone, the void fraction in the unblocked channel is somewhat higher than in the blocked channel. The presence of the blockage promotes mixing between the channels, thus reducing the void differences that may exist between them.

Key Words: subchannels, blockages, void fraction, diversion cross-flow

1. INTRODUCTION

The investigation of the consequences of coolant flow area blockages in fuel assemblies is of great importance for both thermal and fast breeder reactor safety. In pressurized water reactors, during the refilling and reflooding phases of a hypothetical loss-of-coolant accident, the temperature of the zircaloy fuel cladding may reach very high values. These high temperatures coupled with high internal pressures, brought about by gaseous fission products, may trigger a ductile or brittle failure of the cladding. The ductile failure may result in a ballooning of the fuel rod, while with brittle failure the rod may burst open. In both cases, the flow area of a given subchannel or a group of subchannels could be reduced. The grid spacers and, especially in CANDU reactors, the end plates may also perturb the emergency core cooling fluid flow significantly.

One of the consequences of the blockage of a subchannel or a group of subchannels is to divert, depending on the severity of the blockage, some or all of the flow into neighboring unblocked subchannels. The flow recovery downstream of the blockage is a slow process and it may take many hydraulic diameters before the flow is restored to its far upstream value. Therefore, immediately downstream of the blockage, higher enthalpies will prevail in the blocked subchannels than in the unblocked subchannels, and the heat transfer in these regions may be impaired or enhanced due to the turbulence. An adequate prediction of the enthalpies and heat transfer conditions in the downstream region requires detailed information on the flow redistribution caused by the blockage.

The objective of this research is to study the axial distribution of void fractions in two laterally interconnected channels when one of them is blocked at various degrees of severity.

2. LITERATURE SURVEY

Earlier experiments on interconnected channels were intended to obtain data on single-phase unblocked flows. Subchannel mixing caused by turbulence and diversion cross-flow due to the pressure difference between the subchannels have been studied by Hetsroni *et al.* (1968), Skinner *et al.* (1969), Tapucu (1977), Tapucu & Merilo (1977) and Tapucu & Troche (1977). The hydrodynamic behavior or two-phase flows in interconnected channels without blockages has been studied experimentally by Rowe & Angle (1967), Lahey & Schraub (1969), Van Der Ros (1970), Gonzalez-Santalo (1971), Singh (1972), Tsuge *et al.* (1979) and Tapucu *et al.* (1986a). Recently, the effects of the flow orientation on the two-phase flow distribution have been investigated by Shoukri *et al.* (1984), Sato & Sadatomi (1985) and Tapucu *et al.* (1986b).

Experiments on two-phase flow in interconnected channels with blockage in one of them are, to the best of the authors' knowledge, very limited. However, a great deal of data have been reported (Stiefel & Nothiger 1969; Stiefel 1971, 1972; Rowe *et al.* 1973; Vegter *et al.* 1974; Creer *et al.* 1979; Tripe & Weinberg 1980; Hochreiter *et al.* 1980) under single-phase flow conditions.

Recently, Gençay *et al.* (1984) and Tapucu *et al.* (1984) presented data on mass flow rates and pressures upstream and downstream of blockages of different shapes and severities for single-phase flows. The data have also been compared with the predictions of the COBRA-III-C subchannel code (Rowe 1973). They observed that in the region upstream of the blockage, the diversion cross-flow takes place over a relatively short distance. Downstream of the blockage, the recovery of the diverted flow by the blocked channel is a slow process and the rate of this recovery worsens with increasing blockage severity. For a given blockage fraction, the diversion cross-flow caused by a smooth blockage is smaller than that of a plate blockage. Except for high blockage fractions, the equalization of the pressures in the two channels is a fairly rapid process. The authors have also reported that the COBRA-III-C code predicts the data on 30% plate blockage fairly well. However, the code fails to predict the data on plate blockages of 60% or higher severity. For 60% smooth blockage reasonable predictions have been obtained.

The effect of singularities such as contraction, expansion, combination of contraction and expansion, orifices, inserts etc., on two-phase flows have only been determined in single channels. For all practical purposes, only irreversible pressure losses across the restrictions have been reported (Hoopes 1957; Murdock 1962; Janssen & Kervinen 1964; Weisman *et al.* 1978; Simpson *et al.* 1979, 1983; Fairhurst 1983; Salcudean *et al.* 1983a). Salcudean *et al.* (1983b, c) studied the void fraction distributions and two-phase flow transitions in horizontal air–water flows. Tapucu *et al.* (1988) determined the axial distribution of void fractions and pressures upstream and downstream of plate and cosine-shaped smooth blockages. Visual observation of the blocked region showed that a recirculation zone forms on both sides of the blockage. The upstream recirculation zone is small and rich in liquid, whereas the downstream recirculation zone is large

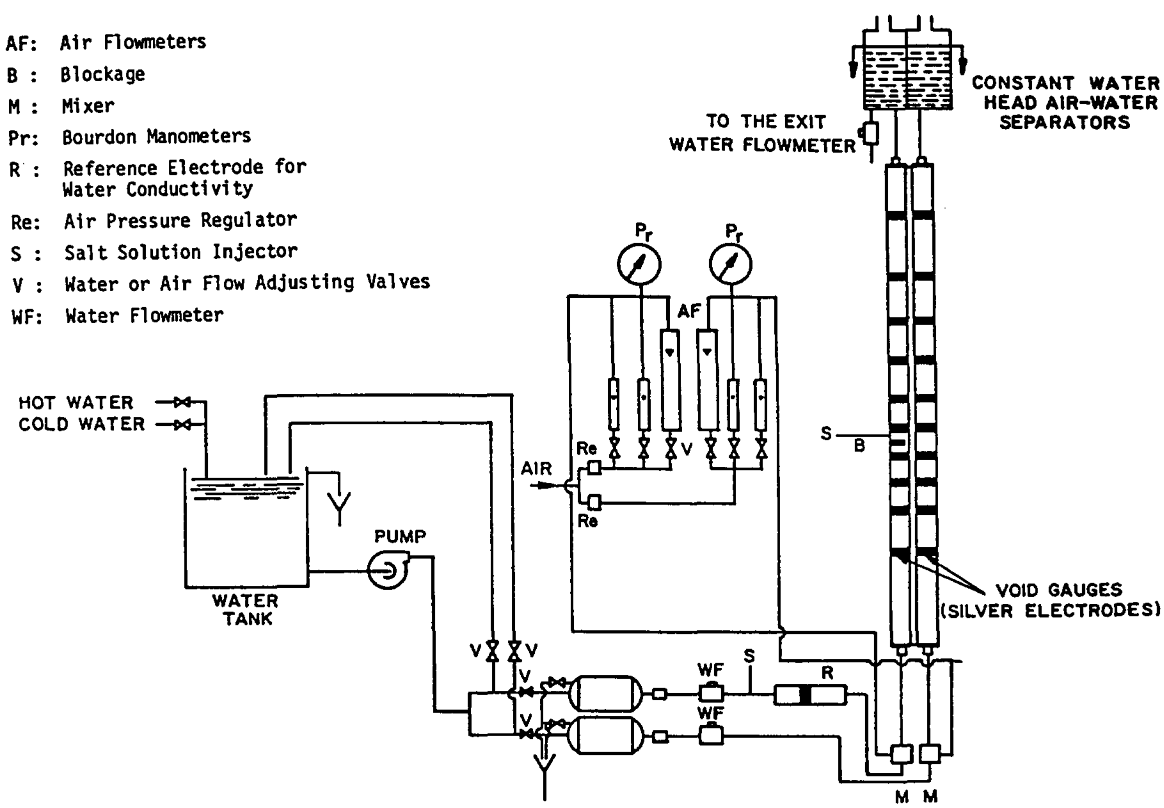

Figure 1. Experimental apparatus.

and has a high void content. Using the irreversible pressure drop data the authors have also determined the contraction coefficient and irreversible pressure loss coefficients.

3. EXPERIMENTAL APPARATUS

The schematic diagram of the apparatus used to perform the blockage experiments is shown in figure 1. The test section (figures 2 and 3) is made up of two 12.65 mm square channels machined from transparent acrylic blocks, which were chosen to allow visual observation of the two-phase flow regimes. The channels are separated by an intermediate plate in which slots were machined with different geometric parameters. The relevant geometric parameters of the test section are given in table 1. Plate and smooth blockages of varying severities were mounted in channel 1 on the wall opposite the interconnection gap, approx. 22 hydraulic diameters downstream of the beginning of the interconnected region.

The water is supplied to the channels with a pump connected to a constant head water tank. The flow rate in the channels is adjusted with valves installed in each branch and in the corresponding bypass circuits. The air is supplied from the mains of the laboratory and regulated by a relieving-type regulator. The mixing of the liquid and the gas phases is accomplished in a mixer. At the outlet of the test section, the two-phase mixture flows into an air–water separator tank which consists of two compartments: one for each channel. The compartments are open to the atmosphere and their water levels are kept constant. The water flow rates at the inlet of each channel and at the outlet of channel 1 after the separator tank are measured with turbine meters with an accuracy better than $\pm 1\%$. The flow rate of the air is measured with rotameters, with an accuracy of $\pm 2\%$ of the full scale.

Since the objective of the present research is to obtain detailed information on the axial distribution of the average void fractions in the channels upstream and downstream of a blockage, they should be measured quickly and simultaneously at several axial locations. Because of the simultaneous nature of the measurement, the impedance technique is suitable for this research. Besides the advantages of simultaneous measurement, direct reading and the relatively low degree of uncertainty in the void fraction determination, the impedance technique also has some disadvantages: it requires lengthy and complex calibration, has rather poor accuracy at high void fractions ($\geqslant 80\%$) and finally, its response depends quite strongly on the temperature of the water and on the amount of dissolved impurities.

With the impedance technique, the values of the void fraction are obtained by measuring the admittance between two parallel plate electrodes (void gauge). The electrodes, 25.4 mm in length, consist of a thin layer of silver paint sprayed onto the opposing faces of the square channels on both sides of the slot (figure 2). There are ten pairs of electrodes along the blocked and unblocked channels and their positions are given in figure 3. The electrodes are distributed along the channels as follows: one pair before the beginning of the interconnected region, three pairs upstream of the blockage and six pairs downstream of the blockage.

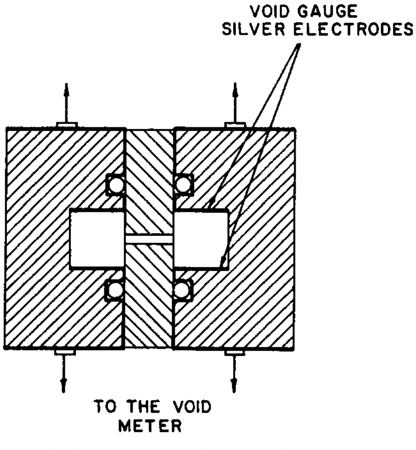

Figure 2. Cross-sectional view of the test section.

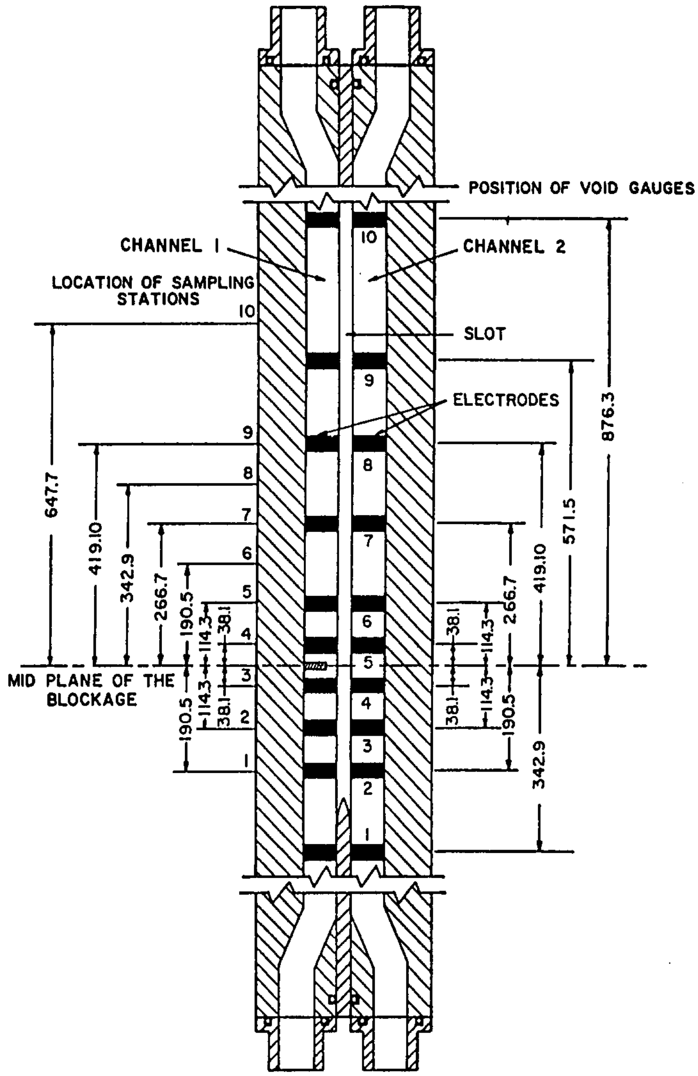

Figure 3. Positions of the void gauges (electrodes) and tracer sampling stations.

Table 1. Geometric parameters of the test section

Gap clearance (mm)	1.5
Gap thickness (mm)	3.2
Hydraulic diameters (mm)	
Channel 1	12.7
Channel 1[a]	12.4
Channel 2	12.8
Channel 2[a]	12.6
Cross-sectional area (mm^2)	
Channel 1	160.0
Channel 1[a]	162.4
Channel 2	163.1
Channel 2[a]	165.5
Length of the interconnection (mm)[b]	1312.0

[a]Including half of the interconnecting gap.
[b]The mid-plane of the blockage is located 272 mm downstream of the beginning of the interconnection.

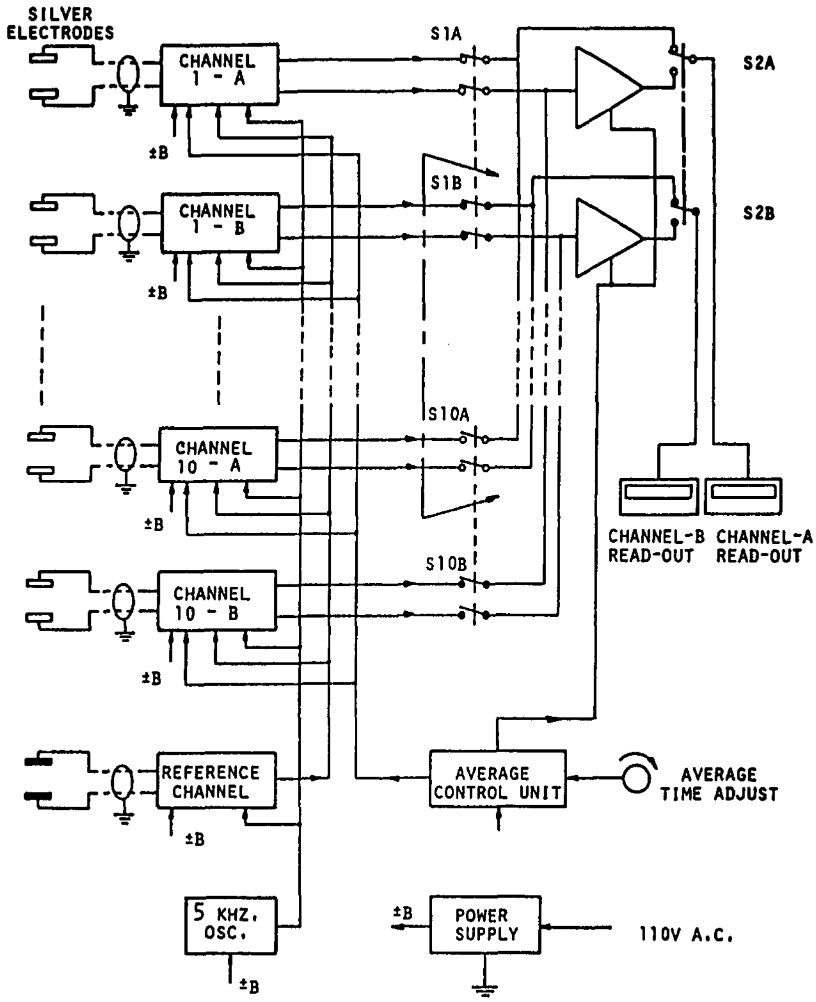

Figure 4. Block diagram of the void fraction measurement system.

Figure 4 shows the block diagram of the void fraction measurement system. Each pair of electrodes is equipped with its own electronic circuit (designed and manufactured by Auburn International Inc.) which monitors the admittance between the plates. A block diagram of the electronic circuit associated with each electrode is given in figure 5. Since all the electrodes are immersed in the same conductive medium, special care must be taken to ensure that no cross-conduction (resistive or reactive) occurs between the measuring channels. The electric isolation of each measuring channel is achieved by coupling transformers excited from a common low impedance 5 kHz oscillator. Also, to avoid a possible current flow through the common power supply, a differential input stage with high common mode rejection and a very high input impedance is used. The voltage drop across the resistance R, mounted between the secondaries of the coupling transformer (figure 5), is a direct function of the current through it. Therefore, it may be assumed that this voltage is also proportional to the admittance between the electrodes, i.e. a function of the liquid fraction between them. To correct for water conductivity variations caused by changes in temperature or impurities, a separate reference channel is used to continuously monitor the admittance of the inlet water (figures 4 and 5). The response of each channel is then divided by the response of the reference, and the errors introduced by the above-mentioned changes are substantially reduced. All the void gauges may be monitored in real time and, when desired, an averaging cycle may be initiated. The averaging period may be set anywhere between 1 and 64 s. After several trials, a 50 s averaging period was found to be optimal for this research. The average value of each channel is measured by a digital voltmeter.

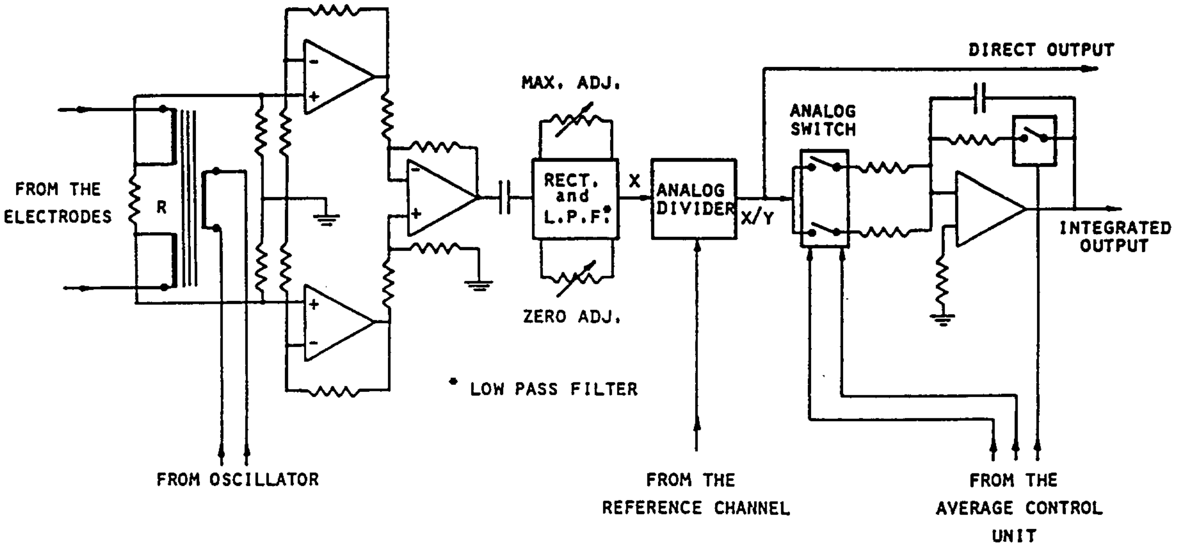

Figure 5. Electronic circuit associated with the void gauges.

The impedance gauges were calibrated by comparing their response to the two-phase mixture flowing through the channel with the average void fraction in the whole channel determined by quick-closing valves. A typical calibration curve is given in figure 6. The liquid mass fluxes ranged between 1000 and 3000 $kg/m^2\,s$. From the calibration curves, it can be concluded that, for the present channel geometry, void fractions up to 80% can be measured with this system. It should be pointed out that each void gauge was calibrated with its associated electronic circuit and connection cables. The main assumption made in the calibration of the void gauges was that the changes in void fraction along the channel caused by the expansion of the gas with decreasing absolute pressure could be ignored. In other words, the void fraction obtained by the quick-closing valve technique adequately represents the void seen by all impedance gauges. This assumption may not be completely true when the gauges are distributed over a long distance (1219 mm in the present research) and when the pressure drop over this distance is not negligible compared to the operating

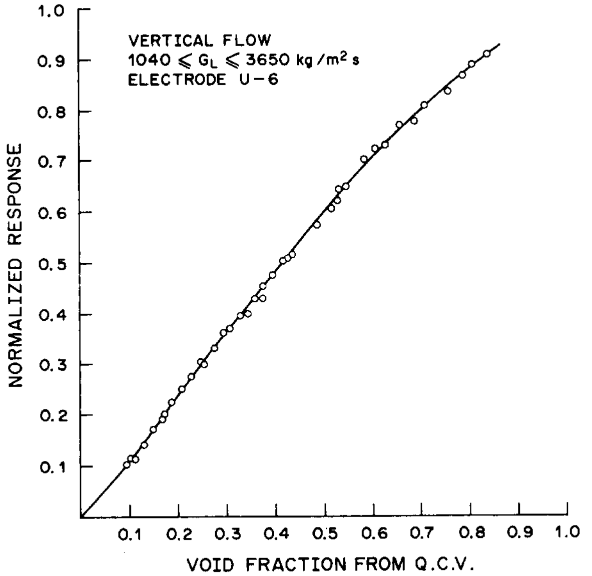

Figure 6. Typical calibration curve of a void gauge (unblocked channel). U-6, electrode No. 6 of the unblocked channel.

pressure of the system. Therefore, the void fraction obtained from the calibration curve of each impedance gauge should be corrected to reflect the real void fraction at a given axial location. The procedure with which the correction was done is described in Tapucu *et al.* (1988). The estimated uncertainty in the void fraction measurements is $\pm 5\%$.

4. BLOCKAGE CONFIGURATION

Two blockage configurations have been studied: plate and smooth (figures 7 and 8). The shape of the latter was a cosine. The plate blockage could be moved continuously in the radial direction to achieve any blockage fraction. Table 2 lists the geometric parameters of the blockages.

5. EXPERIMENTAL RESULTS

Three blockage fractions have been used for plate blockages: 30, 60 and 90%, whereas smooth blockages were limited to blockage fractions of 60 and 90%. For each blockage fraction a set of three experiments was generally conducted:

1. Equal inlet void fractions: 60% at the inlet of each channel,
2. Unequal inlet void fractions with high void at the inlet of the blocked channel: 60 and 0% void fractions at the inlet of the blocked and unblocked channels, respectively,
3. Unequal inlet void fractions with high void at the inlet of the unblocked channel: 0 and 60% void fractions at the inlet of the blocked and unblocked channels, respectively.

In this paper, axial void profiles obtained for 30 and 90% plate blockages, and for a 60% smooth blockage are presented for the groups identified above. More data on void fractions are given in

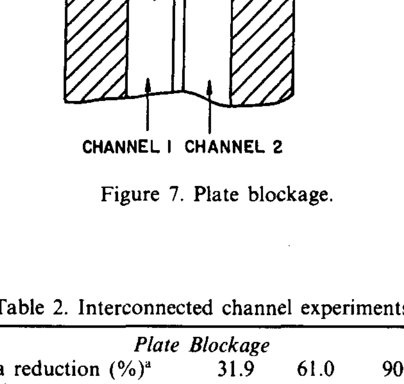

Figure 7. Plate blockage.

Table 2. Interconnected channel experiments

Plate Blockage			
Area reduction (%)[a]	31.9	61.0	90.0
Thickness, L (mm)	3.2	3.2	3.2
Height, h (mm)	4.1	7.9	11.6
Smooth Blockage			
Area reduction (%)[a]	58.0	88.1	
Length, L (mm)	49.9	50.5	
Height, h (mm)	7.5	11.4	

[a]The flow section includes half of the interconnection gap.

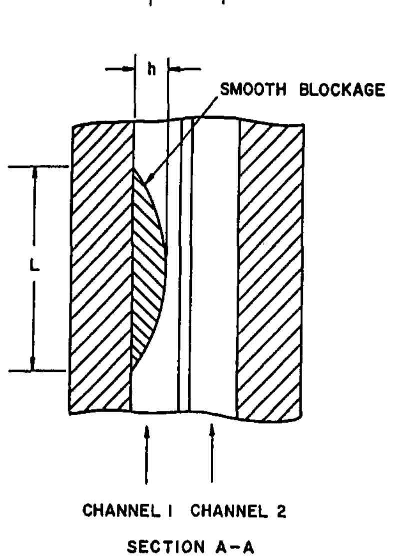

Figure 8. Smooth blockage.

Tapucu *et al.* (1988). Before presenting the experimental results, let us first identify the possible mechanisms which promote flow interchange or mixing between subchannels, as identified by Tahir & Carver (1984):

(1) Turbulent interchange

The salient feature of turbulent motion is that the velocity and pressure at a fixed point do not remain constant with time even in steady state but undergo very irregular high-frequency fluctuations. These fluctuations affect the diffusion of scalar and vector quantities. In the study of mixing in rod bundles, this mechanism by which turbulence enhances diffusion is called "turbulent interchange" (Rogers & Todreas 1972).

In single-phase flow, in the absence of other mixing mechanisms, the subchannel flow remains essentially constant in order to maintain approximately the same pressure level in each subchannel at any axial position. Therefore, in single-phase flow there is momentum and energy transfer between subchannels but there is little or no net mass transfer.

In two-phase flow, in addition to momentum and energy transfer there will probably be a substantial net mass transfer (Gonzalez-Santalo & Griffith 1972).

(2) Diversion cross-flow

Diversion cross-flow is the directed flow caused by pressure gradients normal to the major flow direction. These gradients may be induced by flow section variations caused by blockages, differences in subchannel geometries, gross variation of heat flux or by the onset of boiling in one of the subchannels.

(3) Void drift

This mechanism accounts for the tendency of the vapor phase to shift to higher velocity flow regions. The exact mechanism for this motion is not clear.

(4) Buoyancy drift

In horizontal channels, the void is pushed upward normal to the major flow direction due to the difference in densities between the two phases. The relative significance of this mechanism should diminish at high mass fluxes.

Since the present research deals with vertical flow, the buoyancy drift does not apply. The diversion cross-flow is the major flow interchange mechanism in the blocked region or at the beginning of the interconnected region when the inlet flow conditions in the channels are substantially different. The turbulent interchange and void drift mechanisms govern the mixing between the channels far downstream of the blockage. Moreover, in this paper the term "void migration" will be used to designate the void transfer (i.e. gas transfer) by one or by any combination of the mechanisms identified above.

Equal void fraction at the inlet of the blocked and unblocked channels

For 30% plate blockage, no substantial effect of the blockage on the void fractions in the upstream region is observed until the last measurement point, located at 38.1 mm from the mid-plane of the blockage (figure 9). In the downstream region, the void fraction varies only in the vicinity of the blockage. The somewhat higher void fraction observed in the blocked channel immediately downstream of the blockage is a consequence of bubbles trapped in the recirculation zone which develops behind the blockage. The same phenomenon was also observed in partially blocked single-channel flows by Tapucu *et al.* (1988). Far from the blockage, the void fraction in both channels remains essentially constant, suggesting that the void equilibrium conditions are reached within the length of the interconnected region. The void fractions in the unblocked channel are somewhat higher than those in the blocked channel.

In the 60% smooth blockage the length over which the upstream flow is affected is more visible (figure 10). The void of the recirculation zone behind the blockage is substantial. It is observed

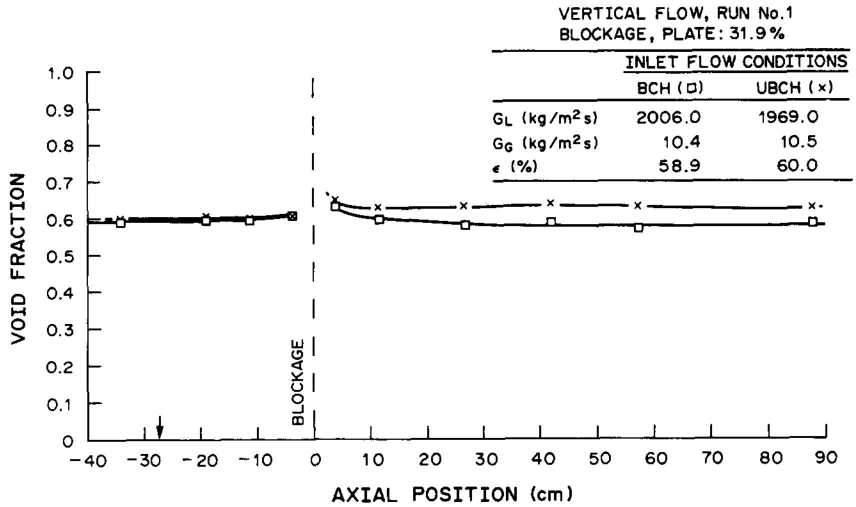

Figure 9. Void fractions in the blocked (BCH) and unblocked (UBCH) channels.

that this zone is limited to the blocked channel only and does not propagate to the unblocked channel. After the recirculation zone, the void fraction in the blocked channel goes through a minimum and then increases slowly towards an asymptotic value. As in the 30% plate blockage, the void fractions in the unblocked channel downstream of the blockage are higher than those in the blocked channel. However, the void equilibrium conditions (almost constant void fraction conditions in the channels) were not reached within the length of the interconnected region. It should be pointed out that the void migration between the channels in the vicinity of the blockage is overwhelmingly due to the diversion cross-flow, while far downstream of the blockage two mechanisms control the void exchange between the channels: turbulent interchange and void drift. Most probably, the blocked channel gains some void with the first mechanism but it loses some void with the second mechanism. When these two mechanisms are balanced, the channels reach their equilibrium void fractions. It is observed that the equilibrium conditions are not those of equal void fraction in each channel: the void fraction in the unblocked channel, as has already been pointed out, is higher than that in the blocked channel. This trend has also been observed in unblocked subchannels by Lahey & Schraub (1969), Gonzalez-Santalo (1971), Tsuge *et al.* (1979) and Shoukri *et al.* (1984).

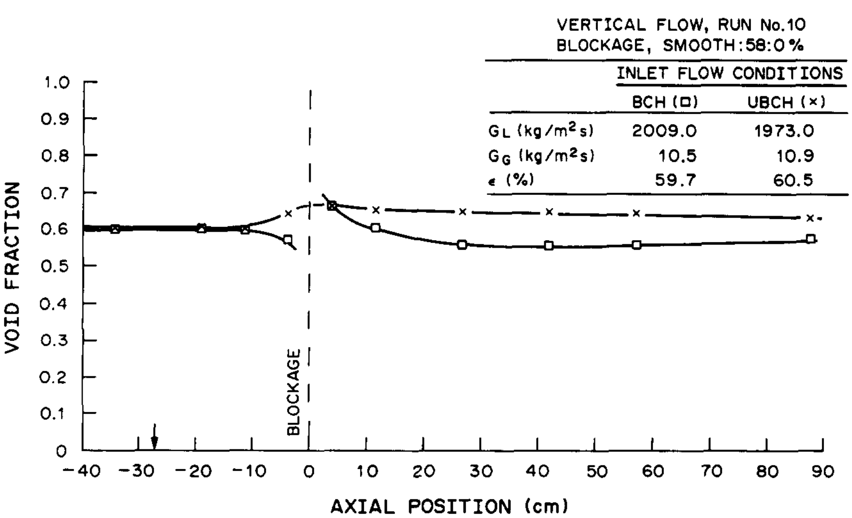

Figure 10. Void fractions in the blocked (BCH) and unblocked (UBCH) channels.

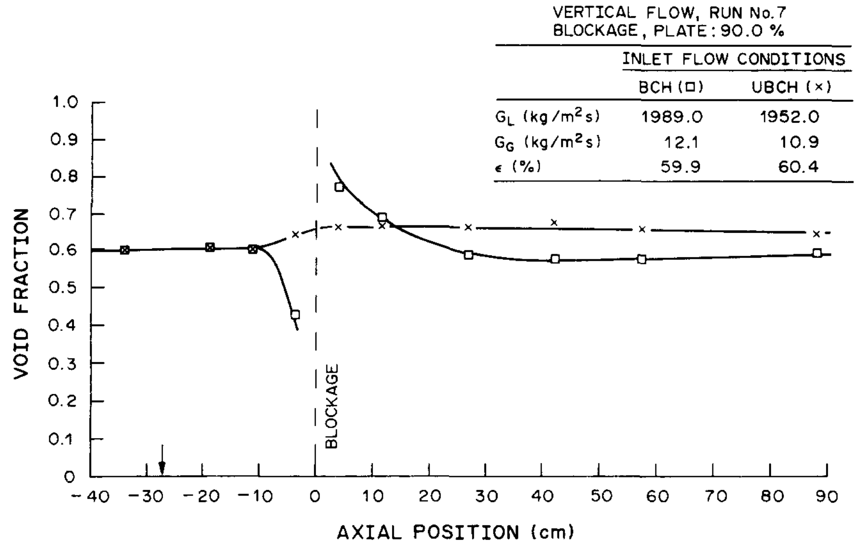

Figure 11. Void fractions in the blocked (BCH) and unblocked (UBCH) channels.

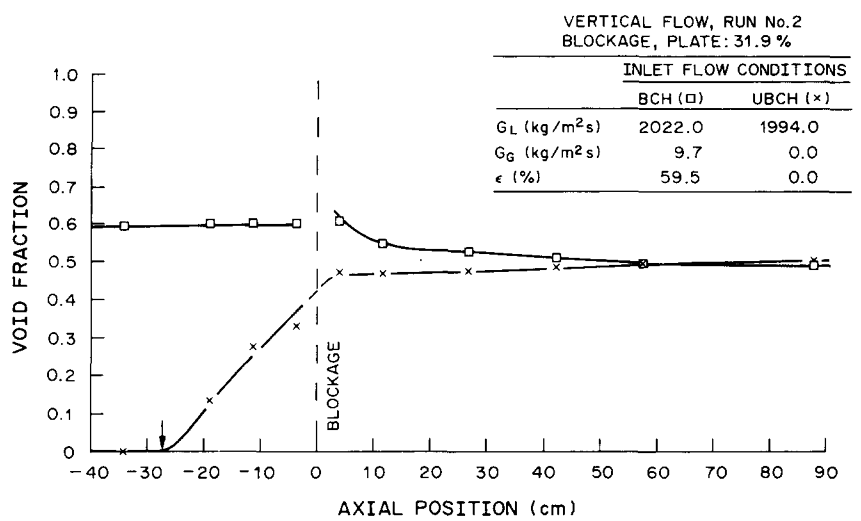

Figure 12. Void fractions in the blocked (BCH) and unblocked (UBCH) channels.

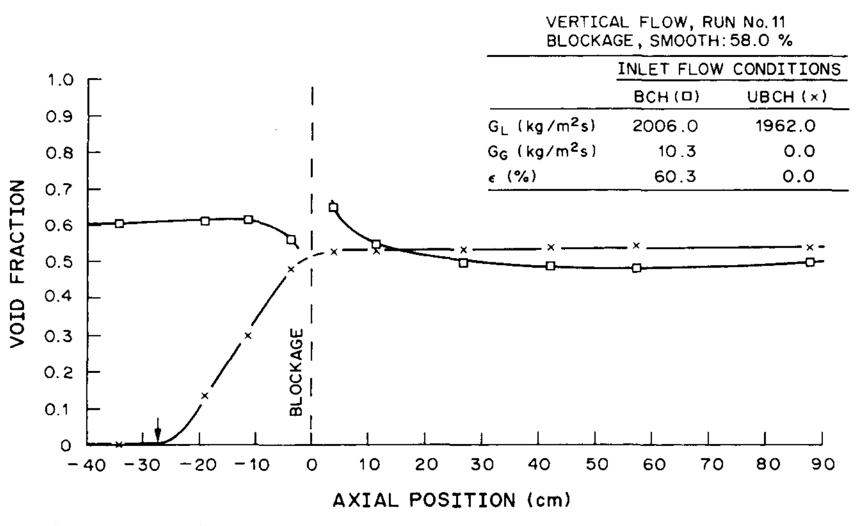

Figure 13. Void fractions in the blocked (BCH) and unblocked (UBCH) channels.

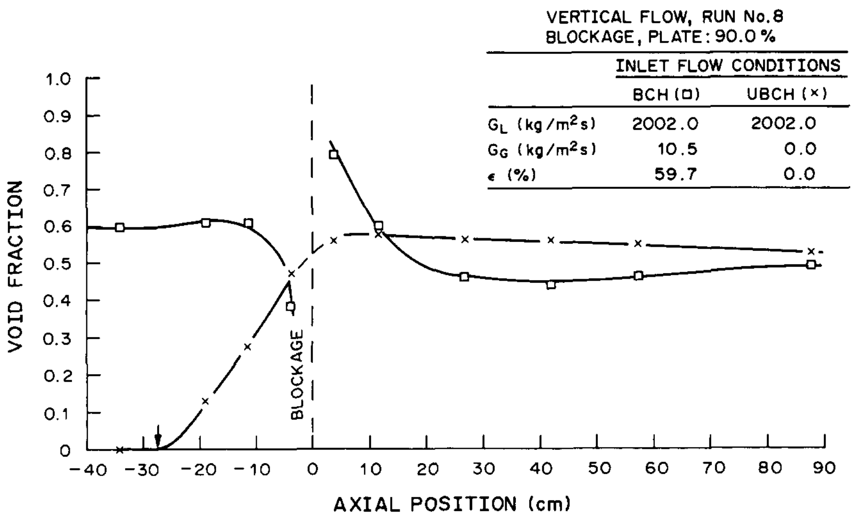

Figure 14. Void fractions in the blocked (BCH) and unblocked (UBCH) channels.

For 90% plate blockage (figure 11), due to the important gas transfer the effect of the blockage was felt 10 hydraulic diameters ($\simeq 120$ mm) upstream of the blockage. Since the gas transfer dominates, the void fraction decreases substantially in the blocked channel and increases in the unblocked channel.

For all blockages, it is observed that a small recirculation zone rich in liquid forms upstream of the blockage. The same observation was also made by Tapucu *et al.* (1988) in partially blocked single-channel flows.

Unequal void fraction conditions with high void at the inlet of the blocked channel

In the upstream region, the behavior of the void fraction in the blocked channel for all blockages is quite similar to that obtained for equal void fractions at the channel inlets (figures 12–14). The effect of the blockage on void fraction in this channel is felt as far as 12 hydraulic diameters upstream ($\simeq 140$ mm), depending on the severity of the blockage. The void fraction in the unblocked channel starts increasing right after the beginning of the interconnected region. This increase is due mainly to the void migration caused by turbulent void diffusion and diversion cross-flow. Figure 15, from Tapucu & Gençay (1984), illustrates the variation of the void fractions in two laterally interconnected channels without blockage for the inlet conditions given in the figure. Due to the migration, the void fraction in the low void channel increases steadily. This migration slows down substantially when the void difference between the channels decreases. By comparing the void fractions in the unblocked channel far upstream of the blockage with those of the low void channel in figure 15 right downstream of the beginning of the interconnected region, the similarity in behavior can easily be observed. The high void is still present immediately downstream of the blockage and its importance increases with increasing blockage severity. Except for 30% blockage, void fractions in the unblocked channel after approx. 8 hydraulic diameters ($\simeq 100$ mm) downstream from the blockage are higher than those in the blocked channel (figures 13 and 14). For 30% blockage (figure 12), the unblocked channel assumes slightly higher void fractions far from the blockage (50 hydraulic diameters or 600 mm).

Unequal void fraction conditions with high void at the inlet of the unblocked channel

For 30% blockage, the void fraction increase observed in the far upstream region in the blocked channel is the consequence of void migration from the high void channel to low void channel (figure 16). When the effect of the blockage is felt, the increase in void fraction slows down substantially. In the unblocked channel, the void fraction remains essentially constant; the slight decrease observed upstream of the blockage could be attributed mainly to the liquid transferred from the blocked to the unblocked channel. In the downstream region, the void fraction in the blocked channel increases steadily to reach an asymptotic value and the recirculation region does

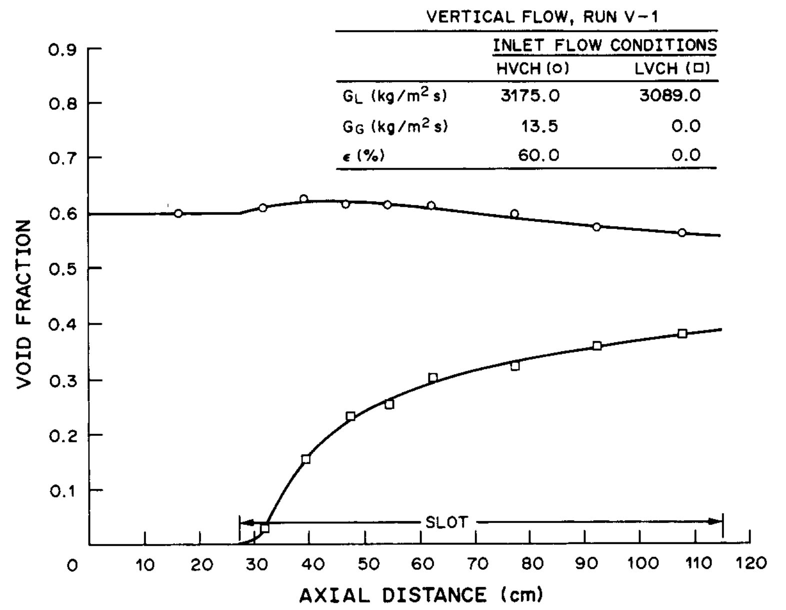

Figure 15. Variation of the void fraction in two laterally interconnected channels without blockage (Tapucu & Gençay 1984). HVCH = high void channel, LVCH = low void channel.

not have a high void content. In the unblocked channel, the void fraction decreases very slowly and its value is higher than that of the blocked channel.

For 60% smooth and 90% plate blockages, upstream of the blockage, the blocked channel loses a substantial portion of the void it gained by void migration (figures 17 and 18). Downstream of the blockage, a high void recirculation zone in the blocked channel is again observed. As usual the void fraction in the unblocked channel is higher than that in the blocked channel.

6. SUMMARY OF THE OBSERVATIONS

The following observations can be made concerning void fraction:

1. In the upstream region, the distance over which the effect of the blockage is felt increases with increasing blockage severity. For a 90% blockage, the extent of this region is approx. 120 mm (10 hydraulic diameters).

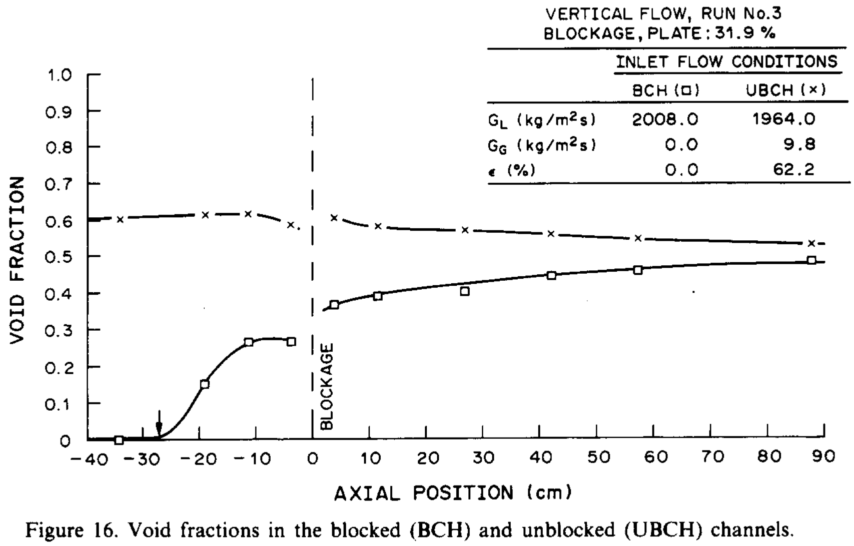

Figure 16. Void fractions in the blocked (BCH) and unblocked (UBCH) channels.

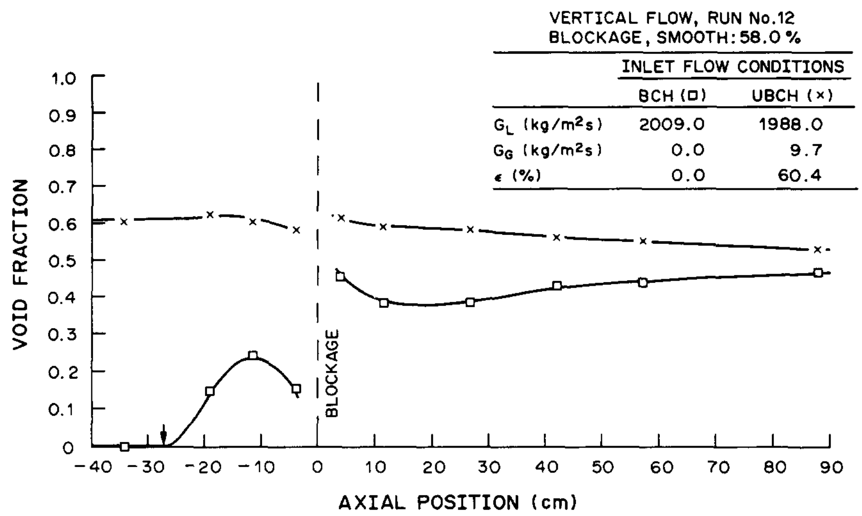

Figure 17. Void fractions in the blocked (BCH) and unblocked (UBCH) channels.

2. Since the gas phase is easily diverted by the blockage, a small recirculation zone rich in liquid develops immediately upstream of the blockage.
3. A high void region develops in the blocked channel right downstream of the blockage. This region is the result of the bubbles trapped in the recirculation zone behind the blockage where low pressures prevail.
4. The extent and the void content of the recirculation zone increases with increasing blockage severity.
5. In the downstream region, the void fraction in the unblocked channel is in most cases higher than that in the blocked channel.
6. The behavior of the void fraction in the channels does not seem to be influenced greatly by the shape of the blockage.
7. When there are substantial void fraction differences between the channels at the beginning of the interconnected region, the effect of the blockage is to equalize them quite efficiently in the downstream region. The void migration induced by void differences between the channels can bring about some equalization of the void between the channels, however, this process is slow and requires long interconnection lengths.

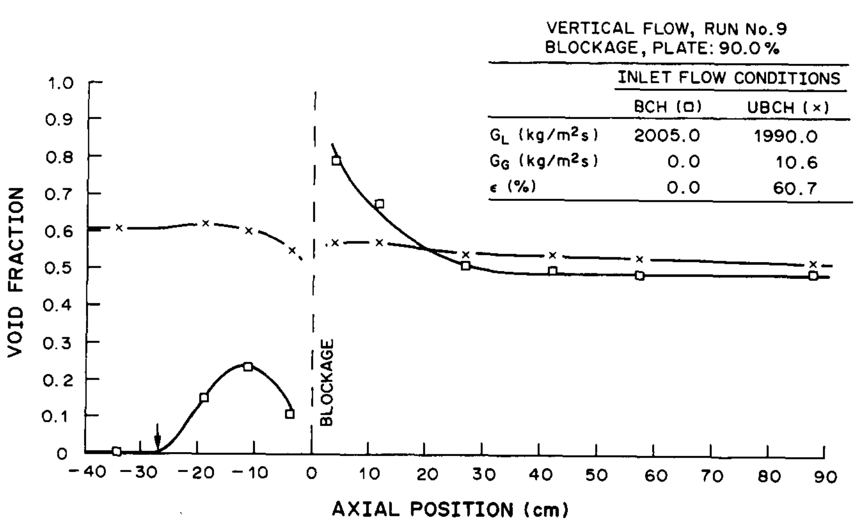

Figure 18. Void fractions in the blocked (BCH) and unblocked (UBCH) channels.

7. CONCLUSIONS

In this research the axial distribution of void fraction in two laterally interconnected channels with blockages in one of them has been determined experimentally. The experiments were conducted on adiabatic two-phase flow which consisted of a mixture of air and water at 20°C. Two blockage configurations have been studied: plate and smooth. The shape of the latter was a cosine.

It is observed that a recirculation zone forms on both sides of the blockage. The upstream recirculation zone is small and rich in liquid, whereas the downstream zone is large and has a high void content. Outside of the downstream recirculation zone, the void fractions in the unblocked channel are somewhat higher than those in the blocked channel. The presence of the blockage promotes the mixing between the channels and rapidly reduces any void difference that may exist between the channels.

Acknowledgements—We are grateful to Mssrs J. C. Juneau and R. Desjardins for their technical contributions. This work was funded by the Electric Power Research Institute, Calif., U.S.A.

REFERENCES

CREER, J. M., BATES, J. M., SUTEY, A. M. & ROWE, D. S. 1979 Turbulent flow in a model nuclear fuel rod bundle containing partial flow blockages. *Nucl. Engng Des.* **52,** 15–33.

FAIRHURST, C. P. 1983 Component pressure loss during two-phase flow. In *Proc. Int. Conf. Physical Modelling of Multi-phase Flow* Coventry, W. Midlands, pp. 1–24.

GENÇAY, S., TAPUCU, A., TROCHE, N. & MERILO, M. 1984 Experimental study of the diversion cross-flow caused by subchannel blockages. Part I—experimental procedures and mass flow rates in the channels. *J. Fluids Engng* **106,** 435–440.

GONZALEZ-SANTALO, J. M. 1971 Two-phase flow mixing in rod bundle subchannels. Ph.D. Thesis, MIT, Cambridge, Mass.

GONZALEZ-SANTALO, J. M. & GRIFFITH, P. 1972 Two-phase flow mixing in rod bundle subchannels. Presented at *ASME Winter A. Mtg*, New York.

HETSRONI, G., LEON, J. & HAKIM, M. 1968 Cross flow and mixing of water between semiopen channels. *Nucl. Sci. Engng* **34,** 189–193.

HOCHREITER, L. E., BASEL, R. A., DENNIS, R. J., LEE, N., MASSIE, H. W., LOFTUS, M. J., ROSAL, E. R. & VALKOVIC, M. M. 1980 PWR flecht seaset 21-rod bundle flow blockage task. Task Plan Report NUREG-CR-1370.

HOOPES, J. W. JR 1957 Flow of steam–water mixtures in a heated annulus and through orifices. *A.I.Ch.E. Jl* **3,** 268–275.

JANSSEN, E. & KERVINEN, J. A. 1964 Two-phase pressure drop across contractions and expansions water–steam mixtures at 600 to 1400 psia. Report GEAP-4622.

LAHEY, R. T. & SCHRAUB F. A. 1969 Mixing, flow regimes, and void fraction for two-phase flow in rod bundles. Presented at *Two-phase Flow and Heat Transfer in Rod Bundles; ASME Winter A. Mtg*, Los Angeles, Calif.

MURDOCK, J. W. 1962 Two-phase flow measurement with orifices. *Trans. ASME Jl Basic Engng* **D84,** 419–433.

ROGERS, J. T. & TODREAS, N. E. 1972 Coolant interchannel mixing in reactor fuel rod bundle, single-phase coolants. Presented at *Symp. Heat Transfer in Rod Bundles*; *ASME Winter A. Mtg*, New York.

ROWE, D. S. & ANGLE, C. W. 1967 Cross flow mixing between parallel flow channels during boiling. Part II. Measurement of flow and enthalpy in two parallel channels. Report BNWL-371, Pt 2.

ROWE, D. S., WHEELER, C. L. & FITZSIMMONS, D. E. 1973 An experimental study of flow and pressure in rod bundle subchannels containing blockages. Report BNWL-1771.

ROWE, D. W. 1973 COBRA IIIC: a digital computer program for steady state and transient thermal analysis of rod bundle nuclear fuel elements. Report BNWL-1695.

SALCUDEAN, M., GROENEVELD, D. C. & LEUNG, L. 1983a Effect of flow obstruction geometry on pressure drops in horizontal air–water flow. *Int. J. Multiphase Flow* **9,** 73–85.

SALCUDEAN, M., CHUN, J. H. & GROENEVELD, D. C. 1983b Effect of flow obstruction on void distribution in horizontal air–water flow. *Int. J. Multiphase Flow* **9,** 91–96.

SALCUDEAN, M., CHUN, J. H. & GROENEVELD, D. C. 1983c Effect of flow obstructions on the flow pattern transitions in horizontal two-phase flow. *Int. J. Multiphase Flow* **9,** 87–90.

SATO, Y. & SADATOMI, M. 1985 Data on two-phase gas–liquid flow distribution in multiple channels. In *Proc. 2nd Int. Conf. Multi-phase* Flow, London, Paper A3, pp. 27–37.

SHOUKRI, M., TAWFIK, H. & CHAN, A. M. C. 1984 Two-phase redistribution in horizontal subchannel flow—turbulent mixing and gravity separation. *Int. J. Multiphase Flow* **10,** 357–369.

SIMPSON, H. C., ROONEY, D. H. & GRATTAN, E. 1979 Two-phase pressure drops in valve and orifice restrictions. Presented at *European Two-phase Flow Gp Mtg,* Ispra, Italy.

SIMPSON, H. C., ROONEY, D. H. & GRATTAN, E. 1983 Two-phase flow through gate valves and orifice plates. In *Proc. Int. Conf. Physical Modelling of Multi-phase Flow,* Coventry, W. Midlands, pp. 25–40.

SINGH, K. 1972 Air–water turbulent mixing in simulated rod bundle geometries. Ph.D. Thesis, Univ. of Windsor, Ontario.

SKINNER, V. R., FREMAN, A. R. & LYALL, H. G. 1969 Gas mixing in rod clusters. *Int. J. Heat Mass Transfer* **12,** 265–278.

STIEFEL, U. 1971 Comparison of measured and calculated mass flow distribution in partially blocked parallel flow channels. EIR Report TM-IN-481.

STIEFEL, U. 1972 Berechnung und Messung des Massequerstromes Zwischem Parallelen Teilkanalen. *Reaktor Tagung, Deutsches Atomforum,* Bonn, Paper 136.

STIEFEL, U. & NOTHIGER, J. 1969 Cross-flow between subchannels. Results of measurements carried out in the MEGAGRE-Rig. EIR Internal Report TM-IN-408.

TAHIR, A. & CARVER, M. B. 1984 Comparison of ASSERT subchannel code with Marviken bundle data. AECL Report AECL-8352.

TAPUCU, A. 1977 Studies on diversion cross-flow between two parallel channels communicating by a lateral slot. I: transverse flow resistance coefficient. *Nucl. Engng Des.* **42,** 297–306.

TAPUCU, A. & GENÇAY, S. 1984 Experimental investigation of mass exchanges between two laterally interconnected two-phase flows. Part I: experimental results on vertical flow. Report IGN-354, Ecole Polytechnique de Montréal, Québec.

TAPUCU, A. & MERILO, M. 1977 Studies on diversion cross-flow between two parallel channels communicating by a lateral slot. II: axial pressure variations. *Nucl. Engng Des.* **42,** 307–318.

TAPUCU, A. & TROCHE, N. 1977 Pressure-induced diversion cross-flow for rod bundle subchannel interconnection geometry. *Trans. Am. nucl. Soc.* **26,** 468–469.

TAPUCU, A., GENÇAY, S., TROCHE, N. & MERILO, M. 1984 Part II—pressures in the channels and the comparison of the COBRA-III-C predictions with experimental data. *J. Fluids Engng* **106,** 441–447.

TAPUCU, A., GEÇKINLI, M., TROCHE, N. & GIRARD, R. 1986a Experimental investigation of mass exchanges between two laterally interconnected two-phase flows. In *Proc. 4th Miami Int. Symp. Multiphase Transport and Particulate Phenomena,* Miami, Fla.

TAPUCU, A., GIRARD, R., TEYSSEDOU, A. & TROCHE, N. 1986b Experimental investigation of void migration between two laterally interconnected two-phase flows, void profiles and effect of liquid mass flux. CDT Project P-1021, Ecole Polytechnique de Montréal, Québec.

TAPUCU, A., TEYSSEDOU, A., GEÇKINLI M. & TROCHE, N. 1988 Experimental study of the diversion cross-flow caused by subchannel blockages. Report EPRI NP-3459, Vol. 2.

TRIPE, G. & WEINBERG, D. 1980 Investigation of turbulent velocity and mass flow distribution in rod bundles with grid-type spacers. Report NUREG-CP-0014, Vol. III, pp. 2189–2203.

TSUGE, A., SAKATA, K. & HIRAO, Y. 1979 Abnormal characteristics of two-phase flow in vertical tube banks. Presented at *ASME Winter A. Mtg,* New York, pp. 139–142.

VAN DER ROS, T. 1970 On two-phase flow exchange between interacting hydraulic channels. Doctorate Thesis, Eindhoven Univ. of Technology, The Netherlands.

VEGTER, B. J., ROIDT, R. M., PECHERSKY, M. J. & MARKLEY, P. A. 1974 Measurement of velocities downstream of a blocked subchannel in a model reactor rod bundle. Westinghouse Research Labs Report No. 74-8E9-RODS-RI.

WEISMAN, J., HUSAIN, A. & HARSHE, B. 1978 Two-phase pressure drop across abrupt area changes and restrictions. In *Proceedings of the Two-phase and Heat Transfer Symposium* (Edited by VEZIROGLU, T. N. & KAKAÇ, S.), pp. 1281–1316. Hemisphere, Washington, D.C.